Available online at www.sciencedirect.com

SciVerse ScienceDirect

Ceramics International 38 (2012) 3741–3745

CERAMICS INTERNATIONAL

www.elsevier.com/locate/ceramint

Single step hydrothermal synthesis of 3D urchin like structures of AACH and aluminum oxide with thin nano-spikes

Muhammad Abdullah *, Mazhar Mehmood, Jamil Ahmad

Department of Metallurgy and Materials Engineering, Pakistan Institute of Engineering and Applied Sciences, Islamabad 45650, Pakistan

Received 20 December 2011; accepted 6 January 2012
Available online 15 January 2012

Abstract

3D urchins like ammonium aluminum carbonate hydroxide (AACH) nanostructures with nano-spikes of dia. 20–30 nm were synthesized by a simple, single step hydrothermal technique by using aluminum nitrate and urea as precursor materials. It was found that morphology of the produced structure strongly depends upon the urea concentration. With increasing the amount of urea, the AACH particles having embedded rods like surface features transformed into 3D urchins. The added urea decomposed during hydrothermal treatment and increased the pH of the solution, which affected the morphology of the produced nanostructures. SEM, XRD, FTIR and TGA were employed to characterize the produced structures. On heating, the volatile ingredients of AACH were removed, leaving behind the alumina urchins.

Keywords: A. Calcination; B. Electron microscopy; B. Whiskers; D. Al_2O_3

1. Introduction

Due to wide range of applications the metal oxides with controlled nanostructured morphologies have drawn considerable attention in the fields of gas-sensing [1], photocatalysis [2], magnetism and energy storage [3,4], high strength composites [5,6], etc. To fabricate nanostructures of various morphologies, numerous techniques have been reported including vapor–liquid–solid (VLS) methods, thermal evaporation, thermal decomposition, chemical vapor deposition (CVD), template-confined and solution-phase methods [7], etc. However, out of these, the solution phase technique is the more promising to obtain nanostructures including nanorods, wires, sheets, flakes, networks, etc. to meet different applications [8]. Out of the other metal oxides, the alumina has a unique position due to its utilization as catalyst, sensor and membrane material [9,10]. Moreover, nano-aluminum hydroxide is further useful due to its sorption–desorption and flame retardation characteristics [11,12].

Presently, a lot of work has been reported on the production of 1D and 2D aluminum hydroxide and alumina nanostructures including nanowhiskers [5,6], nanoflakes [13], nanowires [14], nanofibers [15], nanorods and nanotubes [16], etc. However, the work on 3D nanostructures requires further investigation. Due to their importance 3D nanostructures are also designated as next generation nanostructures [17]. These structures have potential applications in the areas of electronic and optoelectronics [18]. To the best of the authors' knowledge no work on the production of 3D urchin like AACH and aluminum oxide nanostructures synthesized through simple solution based approach has been ever published. Therefore, a facial single-step solution based (hydrothermal) technique to synthesize 3D urchin like AACH and aluminum oxide nanostructures which are composed of fine 20–30 nm spikes, is being reported. Moreover, the possible mechanism for the formation of this nanostructure has also been discussed in this article.

2. Experimental procedures

For the present study, the chemical used were Aluminum Nitrate and Urea. All the chemicals were of analytical grade and were used without any further purification. Series of hydrothermal runs were conducted in which 25 g of aluminum

* Corresponding author. Tel.: +92 51 929 0277; fax: +92 51 922 3727.
E-mail addresses: mabhutta_99@yahoo.com, mabhutta99@gmail.com (M. Abdullah).

0272-8842/$36.00
doi:10.1016/j.ceramint.2012.01.019

Table 1
Synthesized samples, their identification codes and amount of urea used.

S. no.	Sample designation	Urea amount (g)	pH of the filtrate after hydrothermal treatment
1.	U6	6	7.4
2.	U8	8	7.9
3.	U10	10	8.3

nitrate and varying amounts of urea (as mentioned in Table 1) were mixed in 70 ml of distilled water with the help of magnetic stirrer.

After 30 min of stirring, the solution was transferred into the autoclave reactor (by Buchi Glas Uster, Model ''Limbo 350''). The autoclave was sealed and heated up to 120 °C for 24 h. After 24 h, the autoclave was switched OFF and was allowed to cool with the help of installed automatic water circulation system. At room temperature the product was collected carefully. It was filtered using a filter paper, washed repeatedly with distilled water and then dried in an oven for 24 h at 80–85 °C in air. The samples were characterized through SEM, XRD, TGA and FTIR.

3. Results and discussion

Fig. 1(a–d) shows morphologies of the produced nanostructures in the samples (6U and 8U) containing 6 and 8 g urea. Fig. 1(a and b), SEM images of 6U, shows the particles/clusters with 300–500 nm diameter and length up to 3 μm having rod like surface features joined together longitudinally. These features can be ascribed as the initiation point of the spikes of the urchin. By increasing the amount of urea up to 8 g (Fig. 1c and d) these features become more prominent with separation of their surfaces at the interface. By further increasing the amount of urea up to 10 g (Fig. 2a and b), the formation of complete urchin like morphology having size up to 4 μm with diameter of individual spike as 20–30 nm is observed.

These results suggest that the urea has played a vital role in defining the morphology of the produced AACH nanostructure. Urea is an organic compound that decomposes thermally into ammonia and carbon dioxide [19] at 70–100 °C, the chemical reaction is given in Eq. (1) below,

$$CO(NH_2)_2 + 3H_2O \rightarrow 2NH_4^+ + 2OH^- + CO_2 \quad (1)$$

This ammonia then reacts with the aluminum ions (produced due to hydrolysis of aluminum nitrate) in presence of water vapors and forms AACH ($NH_4Al(OH)_2CO_3$) according to the given below chemical reaction (2),

$$CO_2 + H_2O + NH_4^+ + Al^+ + OH^- \rightarrow NH_4Al(OH)_2CO_3 + H_2O \quad (2)$$

By increasing the amount of urea, the number of produced OH^- ions and the pH of the solution increases [20], as shown in Table 1. This increase in the pH results in increasing the number of nucleation sites and ultimately the particle size decreases. Also in accordance with Von Weimarn's theory, the particle size increases as the concentration of the precipitating agent

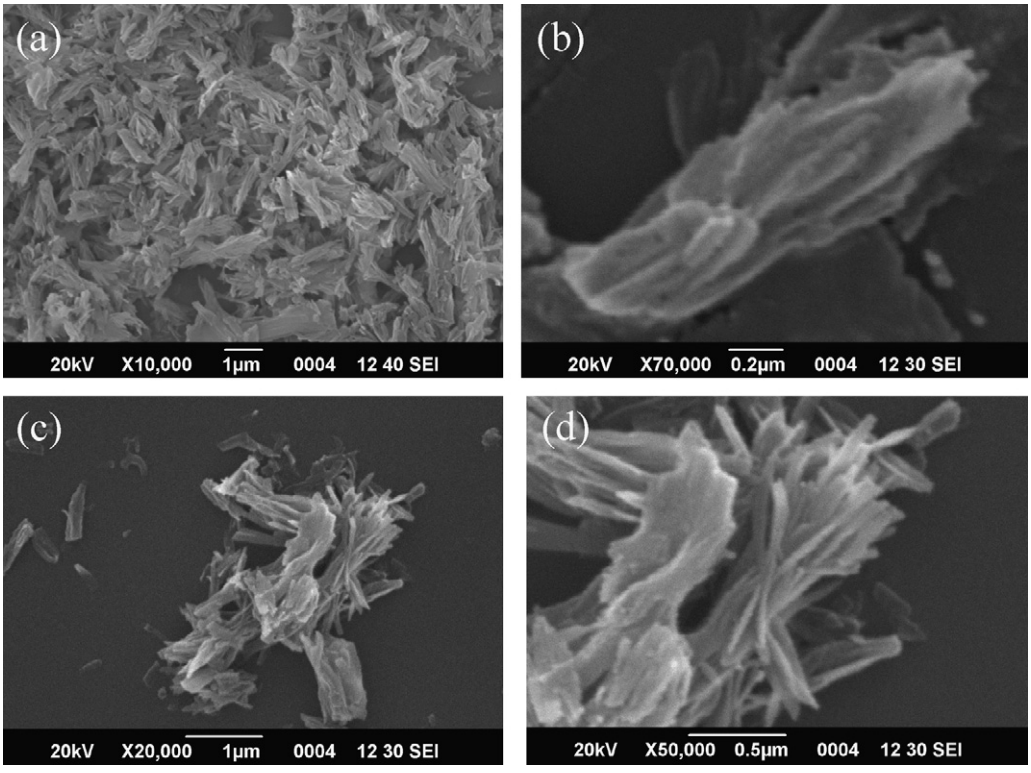

Fig. 1. SEM images of hydrothermally synthesized AACH urchins (a) *U6* low magnification; (b) *U6* high magnification image of individual particle; (c) *U8* low magnification image; (d) *U8* high magnification individual particle.

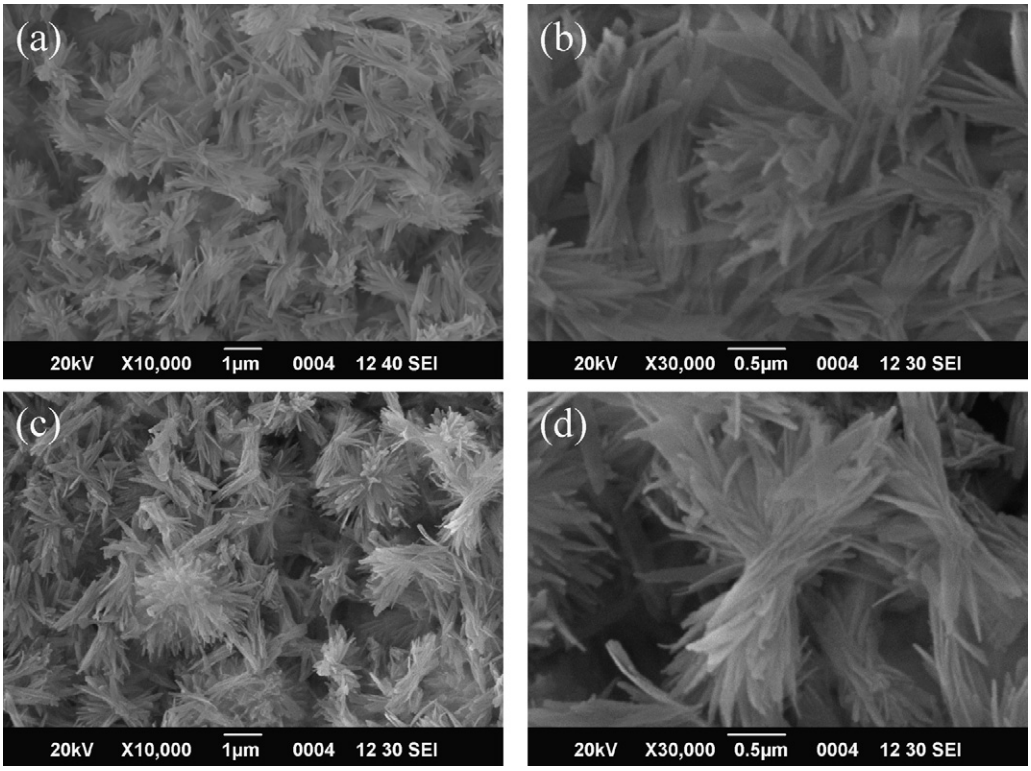

Fig. 2. SEM images of hydrothermally synthesized *U10* AACH urchins (a) low magnification; (b) high magnification; (c) low magnification *U10* urchin calcined at 650 °C; (d) higher magnification image of sample *U10* calcined at 650 °C.

decreases [21]. Therefore, by increasing the concentration of urea the size of the produced structure diminishes, as the energy required for formation of new surfaces becomes available. This results in producing the structure in which the rods like surface morphologies start separating from each other. Even at higher urea concentration, the completely separated whiskers can be produced [6]. The phenomenon has been summarized in Fig. 3(a), which shows the schematics for the formation of urchins. In this figure, it is shown that with increasing the amount of urea the AACH structures undergo three distinct steps. The first is formation of relatively large particles with rod like surface features (U6), second is the small separation of

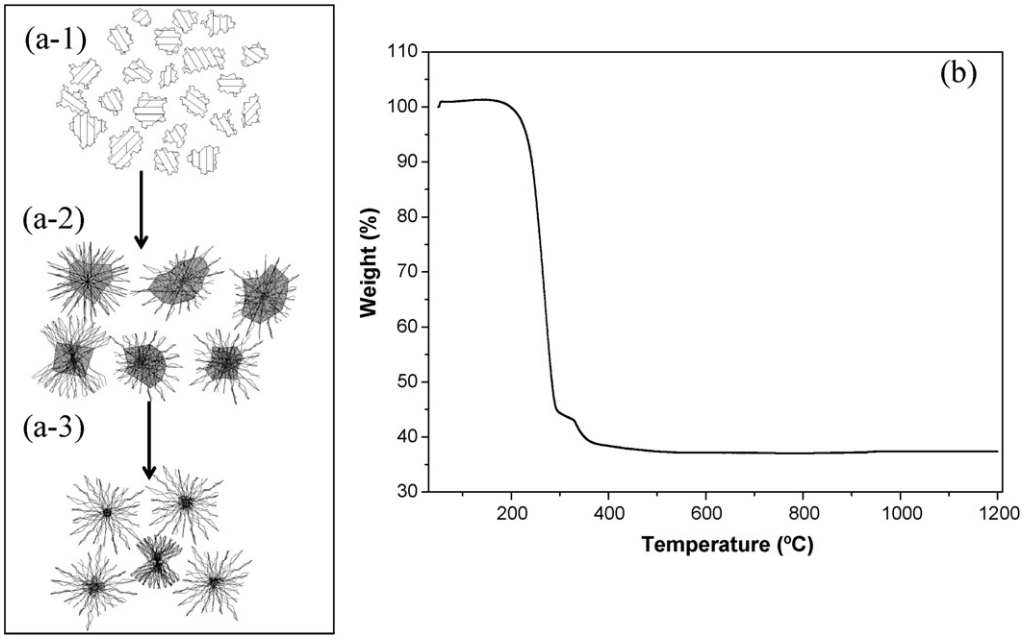

Fig. 3. (a) Schematic illustration of formation of micro-urchins in samples; (a-1) *6U*, (a-2) *8U*, (a-3) *10U*; (b) TGA of *10U* sample.

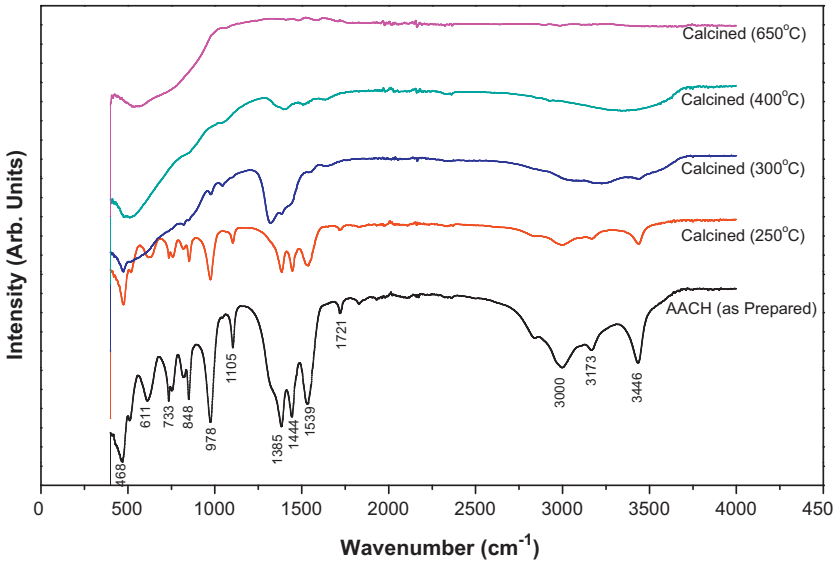

Fig. 4. FTIR image of the *U10* sample uncalcined and calcined at different temperatures.

these rods at the interface (U8) and finally the increase in the separation of these rods and their slight bending at the ends for the formation of urchins (U10) like morphologies.

Fig. 3(b) shows the thermal gravimetric curve of the U10 sample. It shows that complete removal of the volatile species such as carbonates, hydroxides, ammonia and water vapors takes place up to the temperature of 550 °C (approximately). The total weight loss is about 63% which is in good correspondence with [22] the theoretical calculations, i.e.

$$2NH_4Al(OH)_2CO_3 \rightarrow Al_2O_3 + 2NH_3(12.23\,\text{mass loss\%}) + 2CO_2(31.65\,\text{mass loss\%}) + 3H_2O(19.42\,\text{mass loss\%})$$

This shows that the remaining 37% mass is that of the aluminum oxide. As shown in Fig. 2(c and d), as a result of calcinations at the temperature of 650 °C the volatile ingredients of AACH, i.e. NH_3, H_2O and CO_2 are removed and it does not affect the size of the spikes of urchins. So the 63% weight loss has made the nanostructure mesoporous [23], a very important property required for the applications like catalyst.

The urchin shown in Fig. 2, is that of the AACH, this is confirmed with the help of the FTIR (Fig. 4). In this figure the peaks at different wavenumbers indicate the absorptions of infrared wave due to aluminum, hydroxide, ammonia and carbonate groups. Peaks at 3446 and 978 cm^{-1} are due to stretching and bending of hydroxyl group into AACH [24]. The bands at 3000 and 3173 cm^{-1} are due to symmetric and 1385 and 1721 cm^{-1} are due to asymmetric stretching of NH_4^+. Similarly, the bands at 468, 611, 733 and 848 cm^{-1} are ascribed to the vibrational modes of Al–O, while strong band at 1105 cm^{-1} is due to Al–O–Al symmetric vibrations. The peaks at 1444 and 1539 cm^{-1} are due to asymmetric stretching of the bands of CO_3^{-2}.

From Fig. 4, it can be noticed that by calcining at 250 °C, the intensity of almost all the peaks decreases; however, at this temperature no functional group is completely removed. The sharpness of the peaks corresponding to the stretching of OH^-, NH_4^+ and CO_3^{-2} bands further diminishes by calcining the sample at 300 °C. The close observation of the IR spectra of the sample calcined at 300 °C, shows that the sharp peaks corresponding to the vibrational modes of Al–O, diffuse into a broad shoulder in the wave-number range from 400 to 1000 cm^{-1}. This suggests that the crystallinity of the aluminum oxide has diminished and it has transformed to amorphous phase [25,26].

The removal of AACH crystallinity by calcining at 400 °C is also observed through XRD as shown in Fig. 5. From here, it is observed that the as-synthesized structure is that of AACH (JCPDS Card No. 42-0250). By calcining the sample at 400 °C, all its volatile ingredients are removed and left behind is the amorphous alumina. While by calcining the samples at further higher temperature, i.e. 1200 °C, it transforms into α-alumina

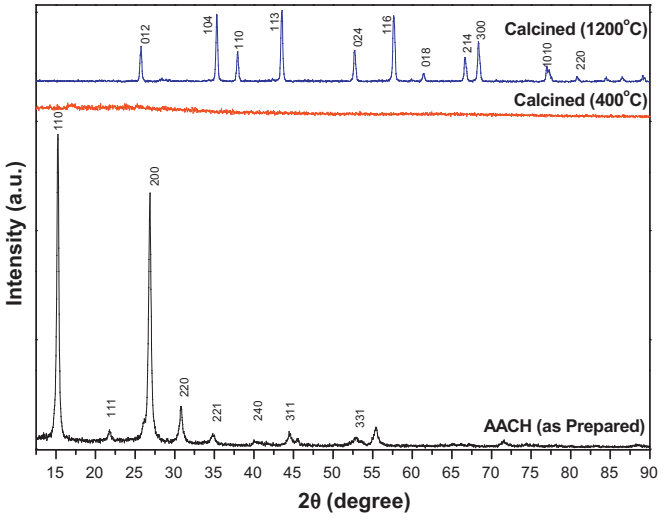

Fig. 5. XRD pattern of *U10* sample uncalcined and calcined at different temperatures.

(JCPDS Card No. 01-010-0173) due to high temperature atomic diffusion.

4. Conclusions

By varying the amount of urea the transformation of microparticles into urchin like morphologies was observed by hydrothermal synthesis technique. In 6 g urea samples, the particles of dia. 300–500 nm and length up to 3 μm with rods like surface features were obtained, by increasing the amount of urea to 8 g. These rods like surface features started to separate into nano-rods at the interface which ultimately result into formation of urchin like morphology in sample containing 10 g urea. The complete removal of volatile ingredients of AACH through calcining the sample at 650 °C and its transformation into amorphous and crystalline α-Al_2O_3 was also confirmed with the help of FTIR and XRD.

Acknowledgement

The financial support from the Higher Education Commission of Pakistan through PhD fellowship (for Muhammad Abdullah) is highly acknowledged.

References

[1] S.Q. Liu, Y.X. Li, M.J. Xie, X.F. Guo, W.J. Ji, W.P. Ding, Y. Chen, Novel hierarchical urchin-like hollow SnO_2 nanostructures with enhanced gas sensing performance, J. Nanosci. Nanotechnol. 10 (10) (2010) 6725–6731.
[2] F. Ksar, G.K. Sharma, F. Audonnet, P. Beaunier, H. Remita, Palladium urchin-like nanostructures and their H_2 sorption properties, Nanotechnology 22 (30) (2011) 305609.
[3] J. Ryu, S.W. Kim, K. Kang, C.B. Park, Synthesis of diphenylalanine/cobalt oxide hybrid nanowires and their application to energy storage, ACS Nano 4 (1) (2010) 159–164.
[4] X.L. Yu, C.B. Cao, X.Q. An, Facile conversion of Fe nanotube arrays to novel alpha-Fe_2O_3 nanoparticle nanotube arrays and their magnetic properties, Chem. Mater. 20 (5) (2008) 1936–1940.
[5] M. Abdullah, J. Ahmad, M. Mehmood, H. Waqas, M. Mujahid, Effect of deflocculants on hardness and densification of YSZ–Al_2O_3 (whiskers & particulates) composites, Compos. Part B: Eng. (2011).
[6] M. Abdullah, J. Ahmad, M. Mehmood, H. Mujtaba ul, H. Maekawa, Synthesis of Al_2O_3 whisker-reinforced yttria-stabilized-zirconia (YSZ) nanocomposites through in situ formation of alumina whiskers, Ceram. Int. 37 (7) (2011) 2621–2624.
[7] C.N.R. Rao, S.R.C. Vivekchand, K. Biswas, A. Govindaraj, Synthesis of inorganic nanomaterials, Dalton Trans. (34) (2007) 3728–3749.
[8] J.Q. Hu, Y. Bando, J.H. Zhan, Y.B. Li, T. Sekiguchi, Two-dimensional micrometer-sized single-crystalline ZnO thin nanosheets, Appl. Phys. Lett. 83 (21) (2003) 4414–4416.
[9] T. Mizushima, K. Matsumoto, J.-i. Sugoh, H. Ohkita, N. Kakuta, Tubular membrane-like catalyst for reactor with dielectric-barrier-discharge plasma and its performance in ammonia synthesis, Appl. Catal. A 265 (1) (2004) 53–59.
[10] C. Yu, G. Liu, B. Zuo, Y. Tang, T. Zhang, A novel gaseous pinacolyl alcohol sensor utilizing cataluminescence on alumina nanowires prepared by supercritical fluid drying, Anal. Chim. Acta 618 (2) (2008) 204–209.
[11] I. Berrodier, F. Farges, M. Benedetti, M. Winterer, G.E. Brown Jr., M. Deveughèle, Adsorption mechanisms of trivalent gold on iron- and aluminum-(oxy)hydroxides. Part 1: X-ray absorption and Raman scattering spectroscopic studies of Au(III) adsorbed on ferrihydrite, goethite, and boehmite, Geochim. Cosmochim. Acta 68 (14) (2004) 3019–3042.
[12] G. Camino, A. Maffezzoli, M. Braglia, M. De Lazzaro, M. Zammarano, Effect of hydroxides and hydroxycarbonate structure on fire retardant effectiveness and mechanical properties in ethylene-vinyl acetate copolymer, Polym. Degrad. Stab. 74 (3) (2001) 457–464.
[13] X.Y. Chen, S.W. Lee, pH-dependent formation of boehmite (γ-AlOOH) nanorods and nanoflakes, Chem. Phys. Lett. 438 (4–6) (2007) 279–284.
[14] J. Zhang, S. Wei, J. Lin, J. Luo, S. Liu, H. Song, E. Elawad, X. Ding, J. Gao, S. Qi, C. Tang, Template-free preparation of bunches of aligned boehmite nanowires, J. Phys. Chem. B 110 (43) (2006) 21680–21683.
[15] H.Y. Zhu, X.P. Gao, D.Y. Song, Y.Q. Bai, S.P. Ringer, Z. Gao, Y.X. Xi, W. Martens, J.D. Riches, R.L. Frost, Growth of boehmite nanofibers by assembling nanoparticles with surfactant micelles, J. Phys. Chem. B 108 (14) (2004) 4245–4247.
[16] H.W. Hou, Y. Xie, Q. Yang, Q.X. Guo, C.R. Tan, Preparation and characterization of gamma-AlOOH nanotubes and nanorods, Nanotechnology 16 (6) (2005) 741–745.
[17] W. Zhou, Z.L. Wang, Three-Dimensional Nanoarchitectures Designing Next-Generation Devices, Springer, 2011.
[18] Y.S. Luo, S.Q. Li, Q.F. Ren, J.P. Liu, L.L. Xing, Y. Wang, Y. Yu, Z.J. Jia, J.L. Li, Facile synthesis of flowerlike Cu_2O nanoarchitectures by a solution phase route, Cryst. Growth Des. 7 (1) (2007) 87–92.
[19] R.E.S. Ii, C. Habeger, A. Rabinovich, J.H. Adair, Enzyme-catalyzed inorganic precipitation of aluminum basic sulfate, J. Am. Ceram. Soc. 81 (5) (1998) 1377–1379.
[20] F. Kara, G. Sahin, Hydrated aluminium sulfate precipitation by enzyme-catalysed urea decomposition, J. Eur. Ceram. Soc. 20 (6) (2000) 689–694.
[21] S.C. Bradford, On the theory of gels, Biochem. J. 15 (4) (1921) 553–562.
[22] Z.S. Wu, Y.D. Shen, Y. Dong, J.Q. Jiang, Study on the morphology of alpha-Al_2O_3 precursor prepared by precipitation method, J. Alloys Compd. 467 (1–2) (2009) 600–604.
[23] Z. Zhu, H. Sun, H. Liu, D. Yang, PEG-directed hydrothermal synthesis of alumina nanorods with mesoporous structure via AACH nanorod precursors, J. Mater. Sci. 45 (1) (2010) 46–50.
[24] K.M. Parida, A.C. Pradhan, J. Das, N. Sahu, Synthesis and characterization of nano-sized porous gamma-alumina by control precipitation method, Mater. Chem. Phys. 113 (1) (2009) 244–248.
[25] C.H. Shek, J.K.L. Lai, T.S. Gu, G.M. Lin, Transformation evolution and infrared absorption spectra of amorphous and crystalline nano-Al_2O_3 powders, Nanostruct. Mater. 8 (5) (1997) 605–610.
[26] K. Morinaga, T. Torikai, K. Nakagawa, S. Fujino, Fabrication of fine alpha-alumina powders by thermal decomposition of ammonium aluminum carbonate hydroxide (AACH), Acta Mater. 48 (18) (2000) 4735–4741.